along a member. R is the axial member force and y the deflection relative to the original member position. Using appropriate boundary and continuity conditions the programme is able to generate the relationship between the applied loading and the rafter angle change in the snap-through bay. A load-angle curve such as that in figure 3.7 is obtained. The apex of this curve is the elastic snap-through buckling load $P_{c\ snap}$.

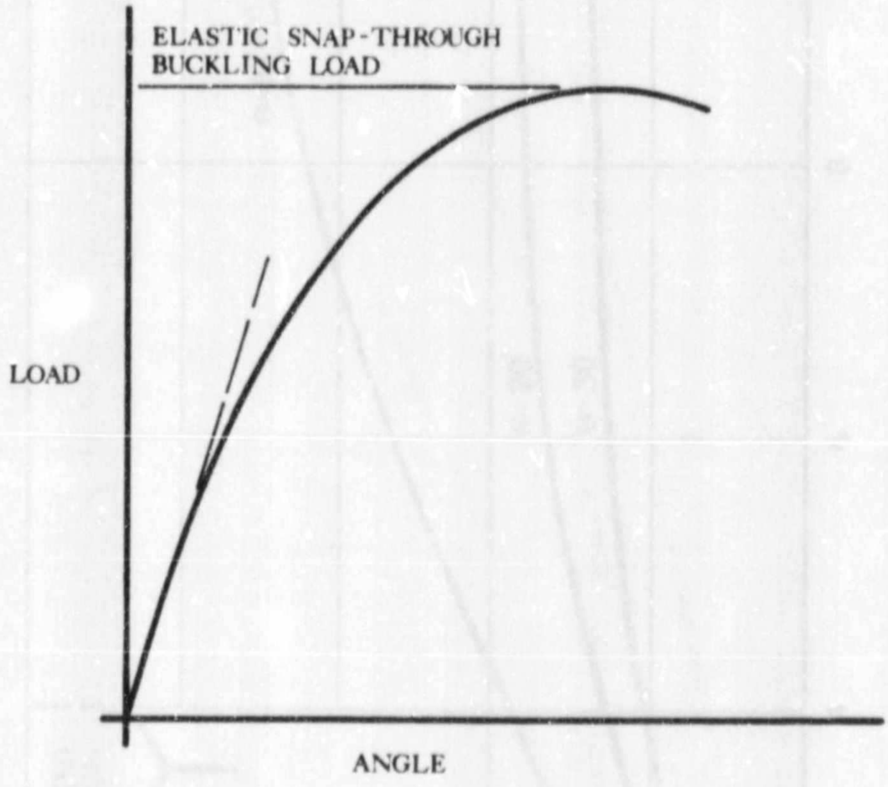

FIGURE 3.7 : LOAD-ANGLE GRAPH

Two sets of analyses were done on the computer, viz:

* Buckling loads were calculated for multi-bay frames under a uniformly distributed load with fixed bases.
* The analysis was repeated for frames with pinned bases.

These results are illustrated in figures 3.8 and 3.9. The effective length factor ℓ/h is depicted as a function of the span to height ratio L/h . From the effective length

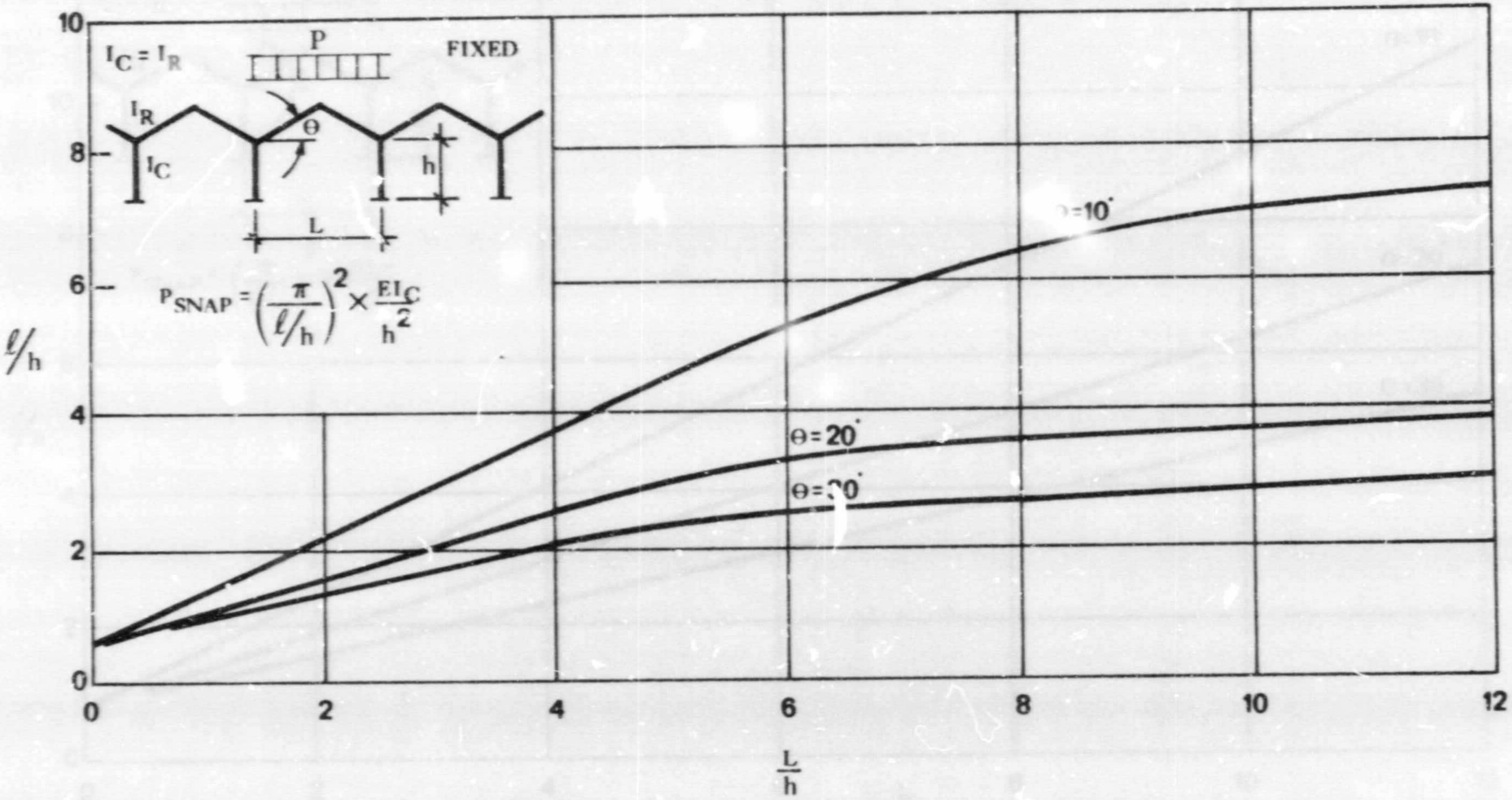

FIGURE 3.8 : ELASTIC SNAP-THROUGH BUCKLING LOADS FOR MULTI-BAY FRAMES WITH FIXED BASES

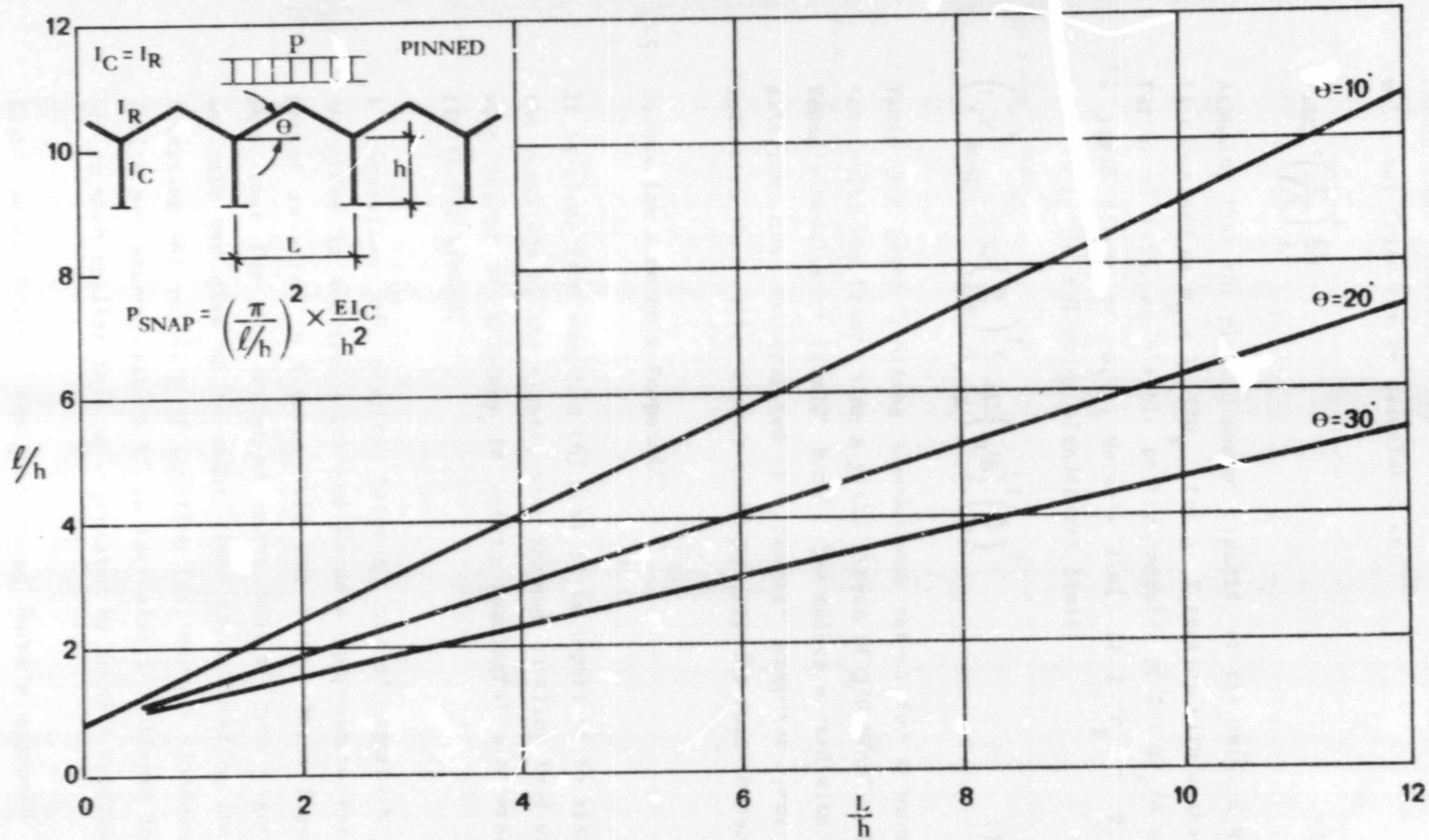

FIGURE 3.9 : ELASTIC SNAP-THROUGH BUCKLING LOADS FOR MULTI-BAY FRAMES WITH PINNED BASES

factor the elastic snap-through buckling load of the multi-bay frame can be calculated as:

$$P_{snap} = \left(\frac{\pi}{\ell/h}\right)^2 \frac{EI_c}{h^2} \qquad (14)$$

Assuming that the plastic moment capacity of the section, M_p, is expressed as $M_p = 1.15Z\sigma_y$ for an I section with a shape factor of 1.15, an elastic section modulus of $Z = 2I_R/d$ and a yield stress of σ_y, Horne's limit of $P_c/P_p \geq 2{,}5A$ results in the following slenderness limit:

$$\left(L/d\right)_{snap} = 1/92\left(\frac{\pi}{\ell/h}\right)^2 \cdot \frac{E}{\sigma_y} \cdot \frac{I_C}{I_R}\left(L/h\right)^2 \cdot \left(\frac{1}{A}\right)^2 \qquad (15)$$

Table 3.2 gives limiting slenderness ratios for a pinned base multi-bay frame using a yield stress of 350 N/mm^2 and a Young's Modulus of 210×10^3 N/mm^2. The values marked with an asterisk are extrapolated as Scholz' computer program indicates that rafter member buckling precedes snap-through.

3.5 Discussion - Horne's Proposals

It is clear from equation (6) that it is important to assess the magnitude of the elastic snap-through buckling load with some degree of accuracy to obtain meaningful slenderness limits for frames.

A comparison of results between Scholz' approach as described in section 3.4.1 and Horne's approximate energy method is given in figures 3.10 and 3.11. These figures show that for the presented cases Scholz' more rigorous analysis can give up to eight times lower buckling loads. Accepting the validity of equation (6), Horne's slenderness limits are unconservative if in fact elastic collapse loads are so much smaller than as calculated by Horne's approach.

Eight model frames, designed using Horne's approach and lying close to the limit of $P_c/P_p = 2{,}5A$ were tested in the

TABLE 3.2 : SCHOLZ' LIMITING SLENDERNESS RATIOS TO PREVENT SNAP-THROUGH FOR PINNED BASE FRAMES $I_C = I_R$

ARCHING FACTOR A	L/h	ANGLE OF RAFTERS		
		10°	20°	30°
1.5	4	29	58	95
	8	33	69	130
	12	36	78	144
2	4	16	33	56
	8	19	39	73
	12	20	43	81
2.5	4	10	21	36
	8	12	25	47
	12	13	28	52
3	4	7	15	25
	8	8	17	33
	12	9	19	36
4	4	4	8	14
	8	5	10	18
	12	5	12	20

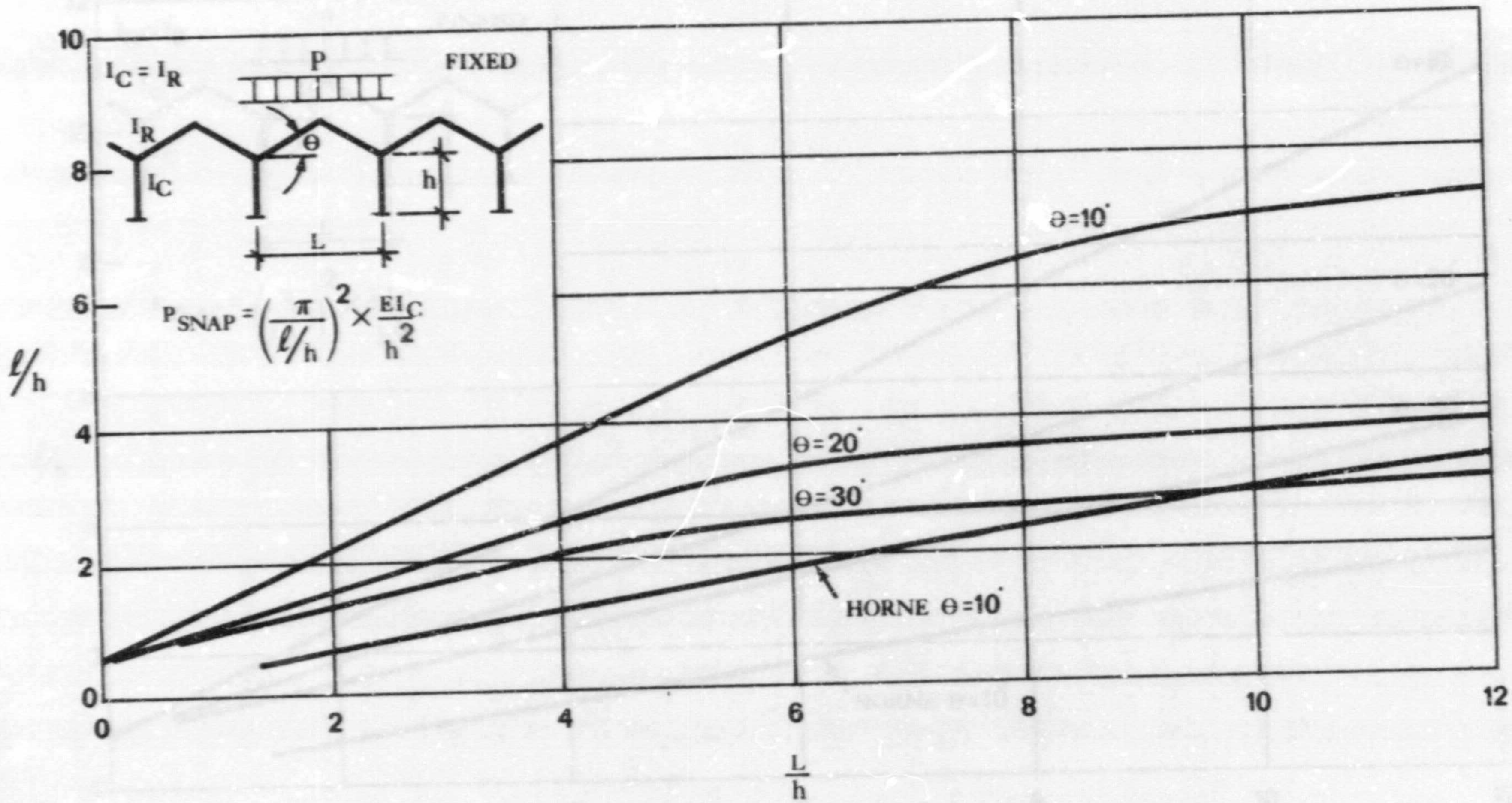

FIGURE 3.10 : COMPARISON OF HORNE'S AND SCHOLZ' SNAP-THROUGH BUCKLING LOADS

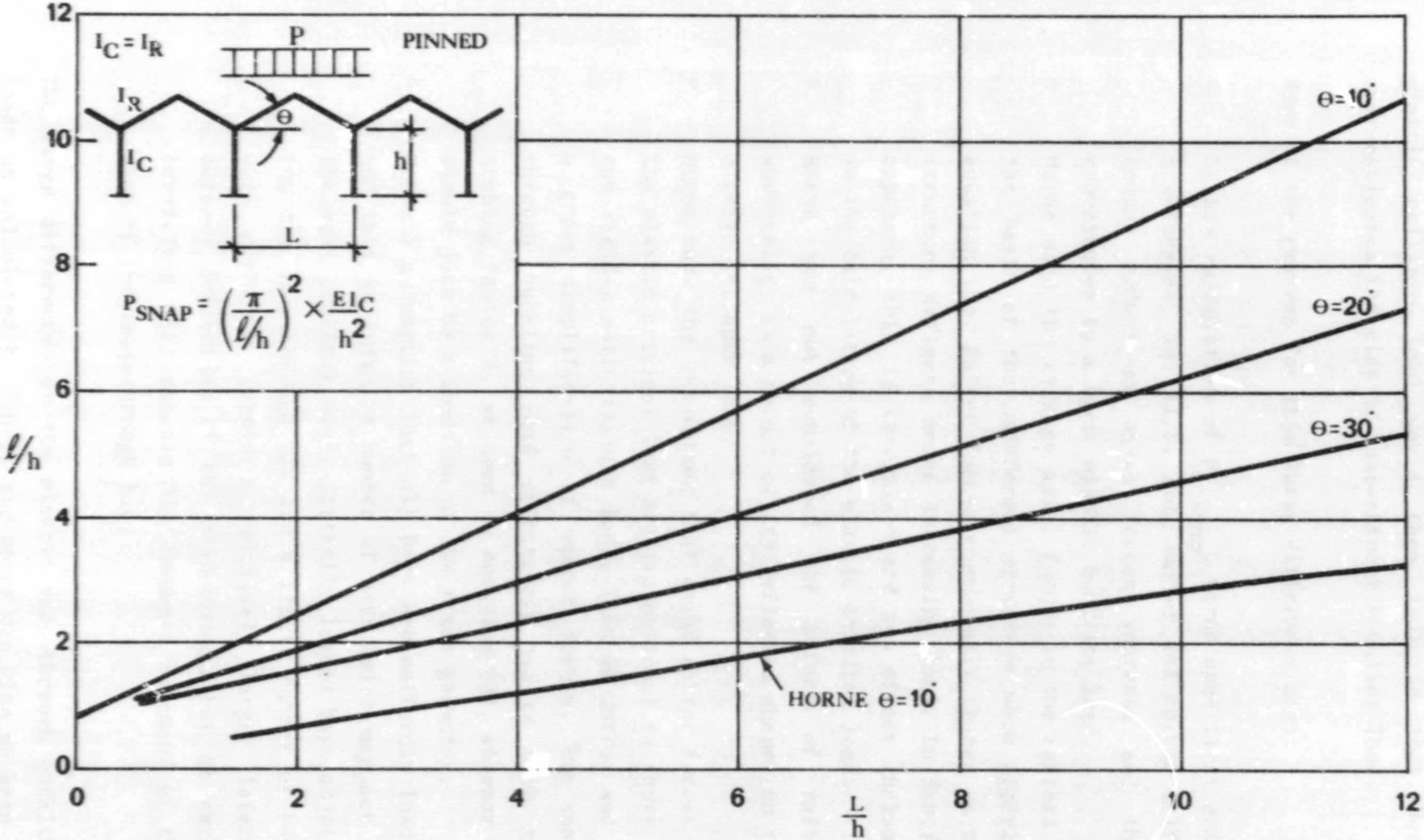

FIGURE 3.11 : COMPARISON OF HORNE'S AND SCHOLZ' ELASTIC SNAP-THROUGH BUCKLING LOADS

laboratory to check this. Failure loads well below the rigid plastic collapse load would then indicate that Horne over-estimates the elastic snap-through buckling load.

Some of the reasons for this large difference are:

* In his calculation of $P_{c\ snap}$, Horne used first order stiffnesses, ie. EI/L. Both rafter and column stiffnesses reduce as axial forces increase and this contributes to a lower elastic buckling load.
* Horne used the average axial forces in the rafters on the basis of the undeformed structure when applying equation (8). Rafter forces continually change as the structure deflects under increasing load. In Scholz' approach, this is recognised and its effect included in the calculation of the elastic critical load.
* Horne has not considered the effect of rafter shortening, as a result of its deflected shape, on the elastic collapse load.
* Horne made the assumption that axial rafter forces at the elastic critical load are proportional to those at the rigid-plastic failure load. This is untrue and is a gross simplification of member forces. The snap-through buckling load effectively varies with the arching factor A, as seen in equation (9), whereas it should just be a function of the frame geometry.
* Horne's assumption that all bays are uniformly loaded and that an infinite number of bays exist may not be the most critical case. Partially loaded bays adjoining the snap-through bay and a finite number of bays will certainly permit a relatively larger lateral outward deflection of the snap-through bay at eaves level.This will enhance the downward movement of the apex of the snap-through bay.

The large differences in the elastic snap-through buckling loads as calculated by Scholz and Horne can also be seen in a comparison of their slenderness limits. This is illustrated in Table 3.3. As stated previously, those values marked with an asterisk indicate that Scholz' computer program predicts individual member instability before the elastic snap-through load is reached.

Also included in the table are slenderness limits of SABS 0162,[3] which if satisfied prevent individual member instability from occurring. This code practically contains Horne's slenderness limits for snap-through, albeit derived in a somewhat different way. However additional limits, as mentioned are imposed to safeguard against individual member instability.This is different to other codes (BS 5950[1]; AISC[10])which use an interaction equation for this purpose. Where the SABS 0162 values are lower than Horne's values, they still exceed Scholz' slenderness limits. This suggests that although the problem is reduced somewhat, snap-through instability may still occur.

A number of small-scale model frames were tested in the laboratory to validate Scholz' analytical work in respect of the elastic snap-through buckling load.[5] Details of the frames are given in figure 3.12. Figure 3.13 illustrates the load-deflection plots of the frames and the predicted snap-through buckling loads. Good agreement exists between experimental and calculated results, the difference nowhere exceeding 15%.

If the validity of equation (6) is accepted, the influence of a smaller than expected elastic snap-through buckling load can be shown on the modified Merchant-Rankine diagram in figure 3.14. A practical multi-bay frame having an arching factor A of, say, two and lying on the limit of $P_{c\,snap}/P_p = 2,5A$, may well in fact have a P_c/P_p ratio of one. This is if the elastic critical buckling is over-estimated as Scholz suggests.

TABLE 3.3 : COMPARISON OF HORNE'S AND SCHOLZ' SLENDERNESS RATIOS TO PREVENT SNAP-THROUGH FOR PINNED BASE FRAMES FOR THE LIMIT 2,5A $I_C = I_R$

ARCHING FACTOR A	L/h	ANGLE OF RAFTERS 10°		20°		30°		SABS 0162
		HORNE	SCHOLZ	HORNE	SCHOLZ	HORNE	SCHOLZ	10°
1.5	4	136	29	313	58	647	95	69
	8	204	33	470	69	970	130	89
	12	272	36	627	78	1293	144	111
2	4	51	16	117	33	242	56	39
	8	76	19	176	39	364	73	60
	12	102	20	235	43	485	81	75
2.5	4	27	10	63	21	129	36	28
	8	41	12	94	25	194	47	46
	12	54	13	125	28	259	52	58
3	4	17	7	39	15	81	25	21
	8	25	8	59	17	121	33	37
	12	34	9	78	19	162	36	48
4	4	8	4	20	8	40	14	13
	8	13	5	29	10	61	18	26
	12	17	5	39	11	81	20	36

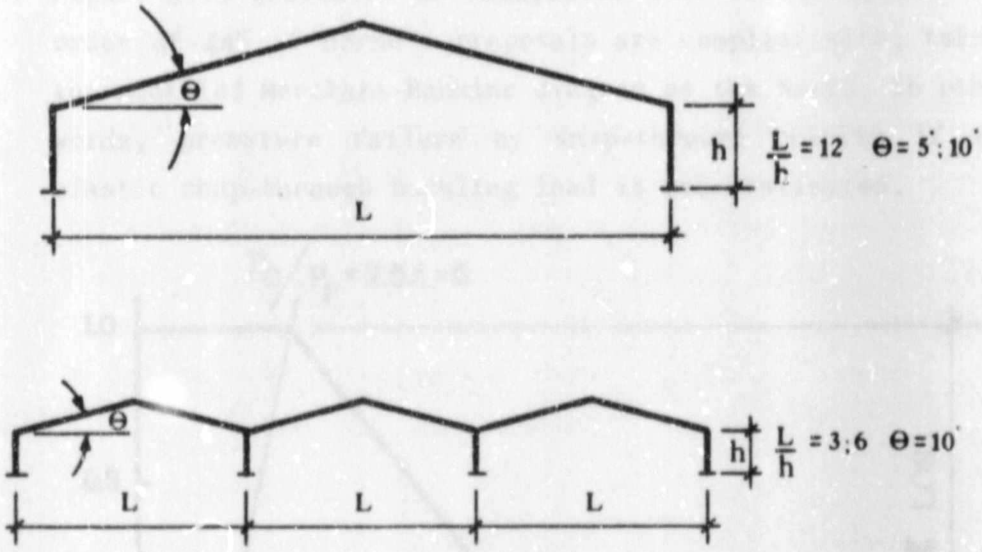

FIGURE 3.12: FRAMES TESTED BY SCHOLZ

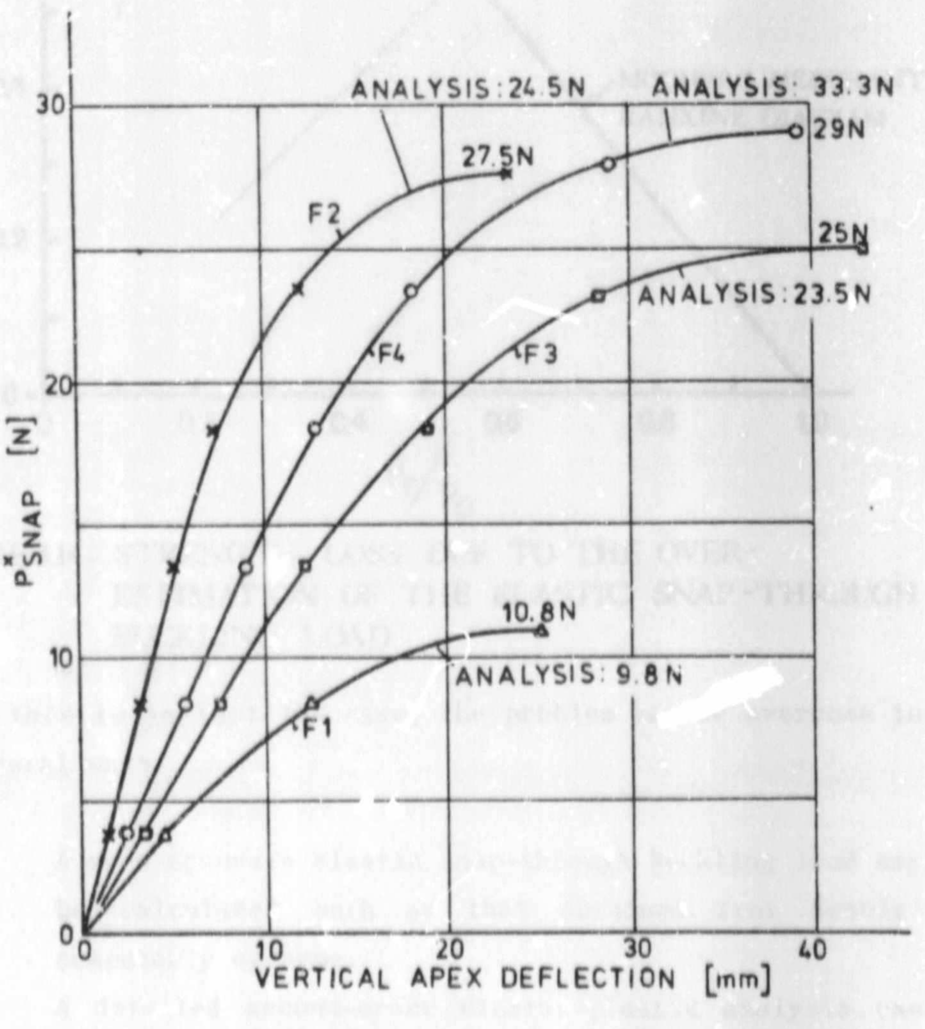

FIGURE 3.13: LOAD-DEFLECTION PLOTS OF FRAMES

Figure 3.14 indicates an unexpected loss of strength of the order of 44% if Horne's proposals are complied with, taking the modified Merchant-Rankine diagram as the basis. In other words, premature failure by snap-through results if the elastic snap-through buckling load is over-estimated.

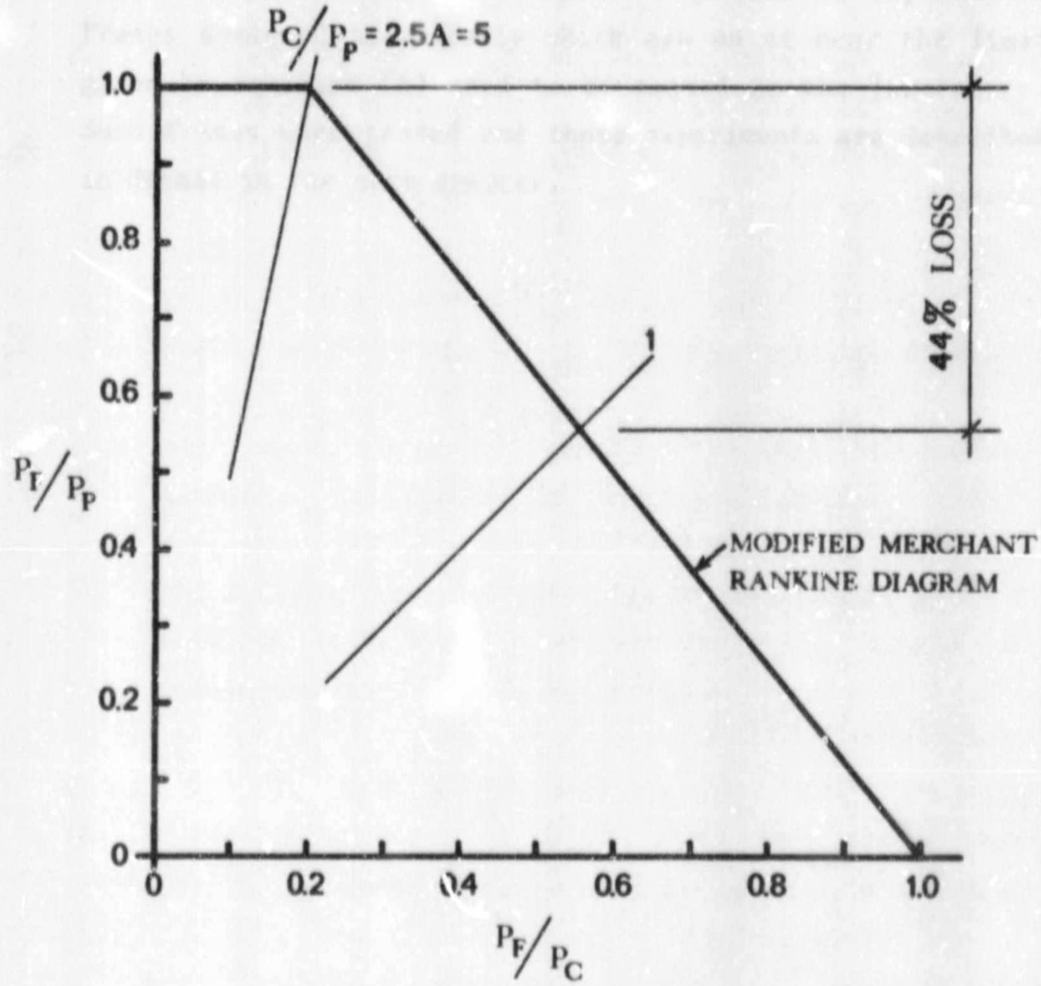

FIGURE 3.14: STRENGTH LOSS DUE TO THE OVER-ESTIMATION OF THE ELASTIC SNAP-THROUGH BUCKLING LOAD

If this is in fact the case, the problem may be overcome in several ways:

* A more accurate elastic snap-through buckling load may be calculated such as that obtained from Scholz' computer programme.
* A detailed second-order elastic-plastic analysis can be undertaken to determine the failure load of the frame.

* Another limit other than that given by equation (11) can be developed.

The question at this stage however, is whether the strength loss, resulting from the over-estimation of the elastic snap-through buckling load can be confirmed by experiment. Frames designed plastically which are on or near the limit given by equation (6) need to be tested in the laboratory. Such frames were tested and these experiments are described in detail in the next chapter.

4. DESCRIPTION OF LABORATORY EXPERIMENTS AND TEST RESULTS

As stated, the question is whether strength loss resulting from premature snap-through instability can be confirmed by experiment. In order to test this the following requirements are made on the experimental frames.

* The geometry of the frames must be such that the ratio of snap-through elastic critical buckling load to rigid-plastic collapse load as calculated by Horne's procedure should be on or close to the proposed limit of 2,5A.
* If any frame instability should occur this should be due to snap-through and not sway instability. In other words $P_{c\ snap}/P_p < P_{c\ sway}/P_p$.
* All other forms of instability such as lateral torsional instability or individual member buckling must be prevented. This is necessary as any reduction in failure load below that of the rigid plastic collapse load can therefore only be caused by unexpected snap-through instability.

It must be noted that the proposed limit of 2,5A in equation (6) is for frames with cladding. Since bare frames were tested in the laboratory, the beneficial effects of cladding were absent. Frame dimensions were therefore chosen giving ratios of $P_{c\ snap}/P_p$ greater than the limit of 2,5A, to ensure that the expected failure loads were close to the rigid-plastic collapse loads.

4.1 Description of Frames

The tested multi-bay pitched-roof portal frames consisted of three bays all of equal span as shown in figure 4.1.

An angle of ten degrees was chosen as snap-through is more pronounced and dominant in frames with a low pitch.

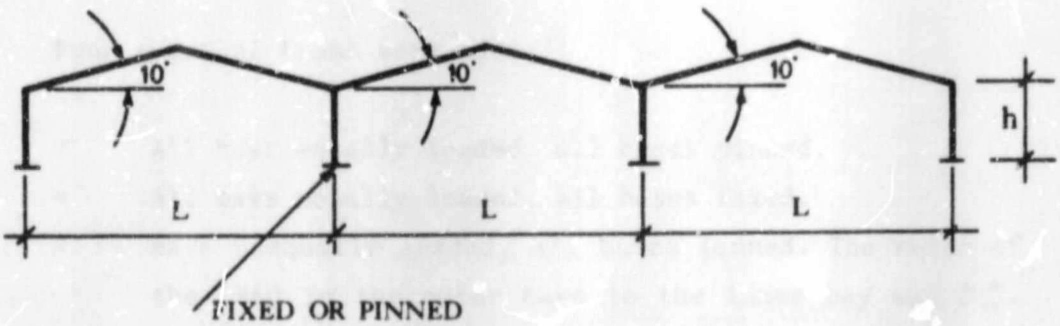

FIGURE 4.1 : FRAMES TO BE TESTED

A uniformly distributed load applied to the rafters in each bay of the frames was simulated by the loading mechanism shown in figure 4.2. The loading as illustrated gives elastic bending moments which are within 4% of those, had a uniformly distributed load been applied. The calculation of the loading points is given in Appendix D.

The loading was applied to each bay, through freely suspended dead weights. This eliminates any interference from friction and permits a clear relationship between a specific load increment and its corresponding displacement. (This is in contrast to a jacking and digital recording system). This is considered to be most important when fairly small loads, such as those used in the experiments, are involved.

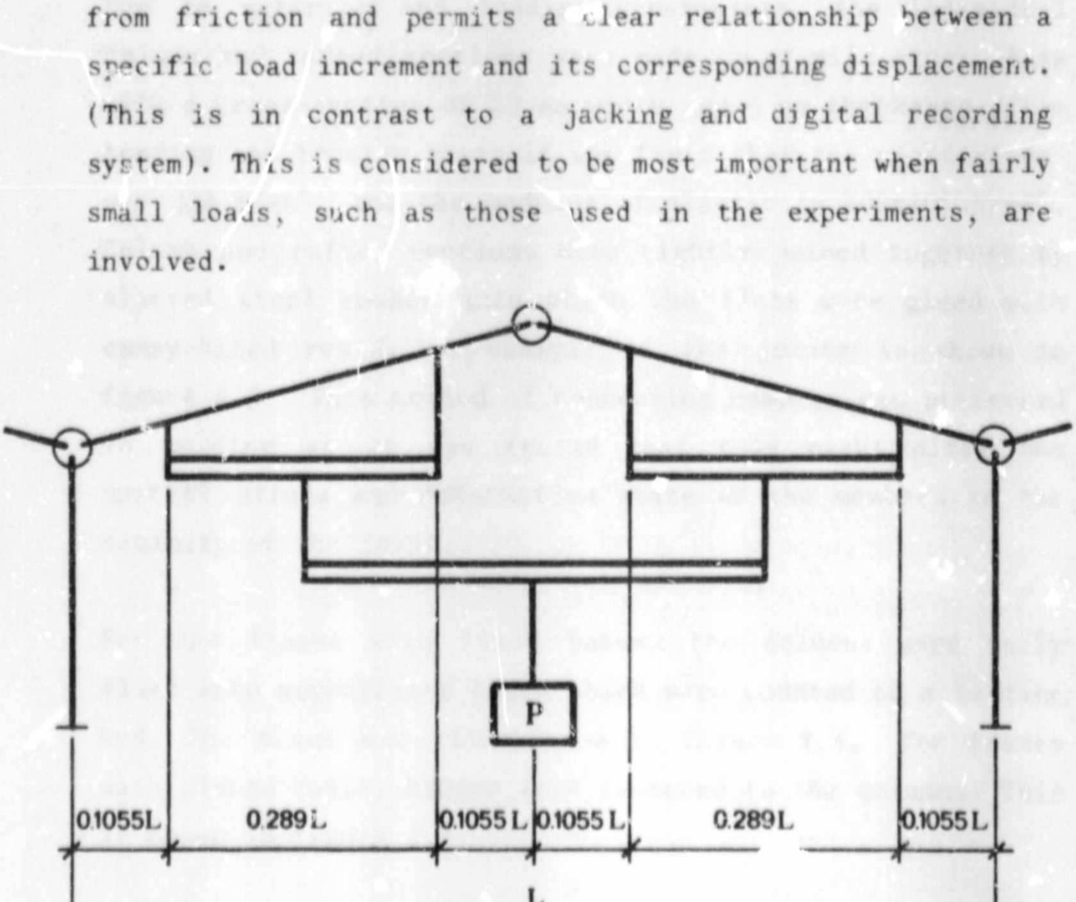

FIGURE 4.2 : LOADING TO SIMULATE A UNIFORMLY DISTRIBUTED LOAD

Four types of frame were tested:

* All bays equally loaded, all bases pinned.
* All bays equally loaded, all bases fixed.
* Bays unequally loaded, all bases pinned. The ratio of the load in the outer bays to the inner bay was 0,7. In practice, this may simulate the difference between the presence and absence of live load.
* Bays unequally loaded, all bases fixed.

Two identical frames within each type were tested. The above experiments were done to test Horne's supposition that a frame with all bays equally loaded and bases pinned gives the worst case. Also, in practice, the situation may well arise that unequal loads are found in adjacent bays.

4.1.1 Materials Used

Due to material and loading constraints, the individual column and rafter sections were made up of mild steel flats with a cross-section of 20 mm width and 5 mm thickness. From bending and tension tests it was found that the yield stress was 334 N/mm^2, and the modulus of elasticity $206x10^3$ N/mm^2. Column and rafter sections were tightly joined together by slotted steel rounds into which the flats were glued with epoxy-based resin. An example of the joints is shown in figure 4.3. This method of connecting members was preferred to welding as it was feared that this might alter the initial stress and deformation state of the members in the vicinity of the joint.

For the frames with fixed bases, the columns were fully fixed into appropriate bases which were mounted on a testing bed. The bases are illustrated in figure 4.4. For frames with pinned bases, hinges were fastened to the columns. This is shown in figure 4.5.

The loading rig was designed so as to apply concentrated loads at the required positions. A layout of the loading rig is given in figure 4.6.

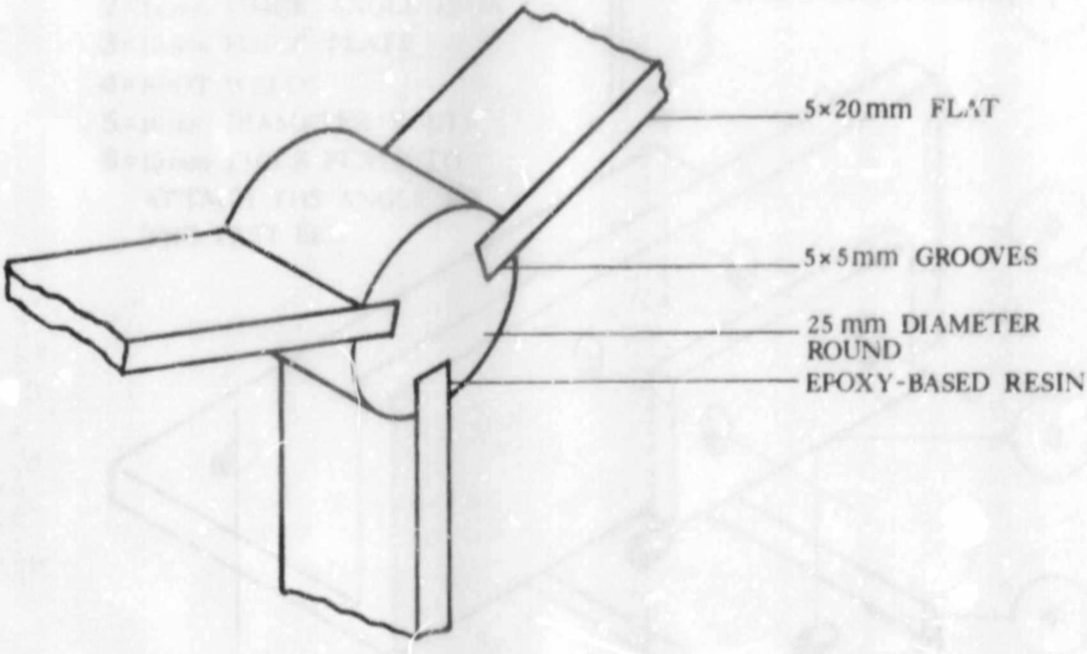

FIGURE 4.3: EXAMPLE OF A JOINT

4.2 Frame Dimensions

Frame dimensions were chosen to satisfy the requirements previously mentioned. Table 4.1 gives the important data for each frame. Column four of table 4.1 gives the calculated rigid-plastic collapse load, applied to the middle bay, of the frame. Column five gives the arching factor A and column six the limit of 2,5A. The ratio of elastic snap-through buckling load to rigid plastic collapse load, of the central bay, as calculated by Equation (8) and applying Horne's assumptions is given in column seven. The same approach is used to calculate the ratio of elastic sway buckling load to rigid plastic collapse load and this value appears in column eight. Calculation of these ratios is given in Appendix E. The following conclusions can be drawn from the table.

* In all cases the calculated ratio of $P_{c\ snap}/P_p$ is greater than the limit of 2,5A. Hence if this limit is correct the actual failure load should be close to the plastic collapse load. However, it must be remembered that bare frames were tested in the laboratory and

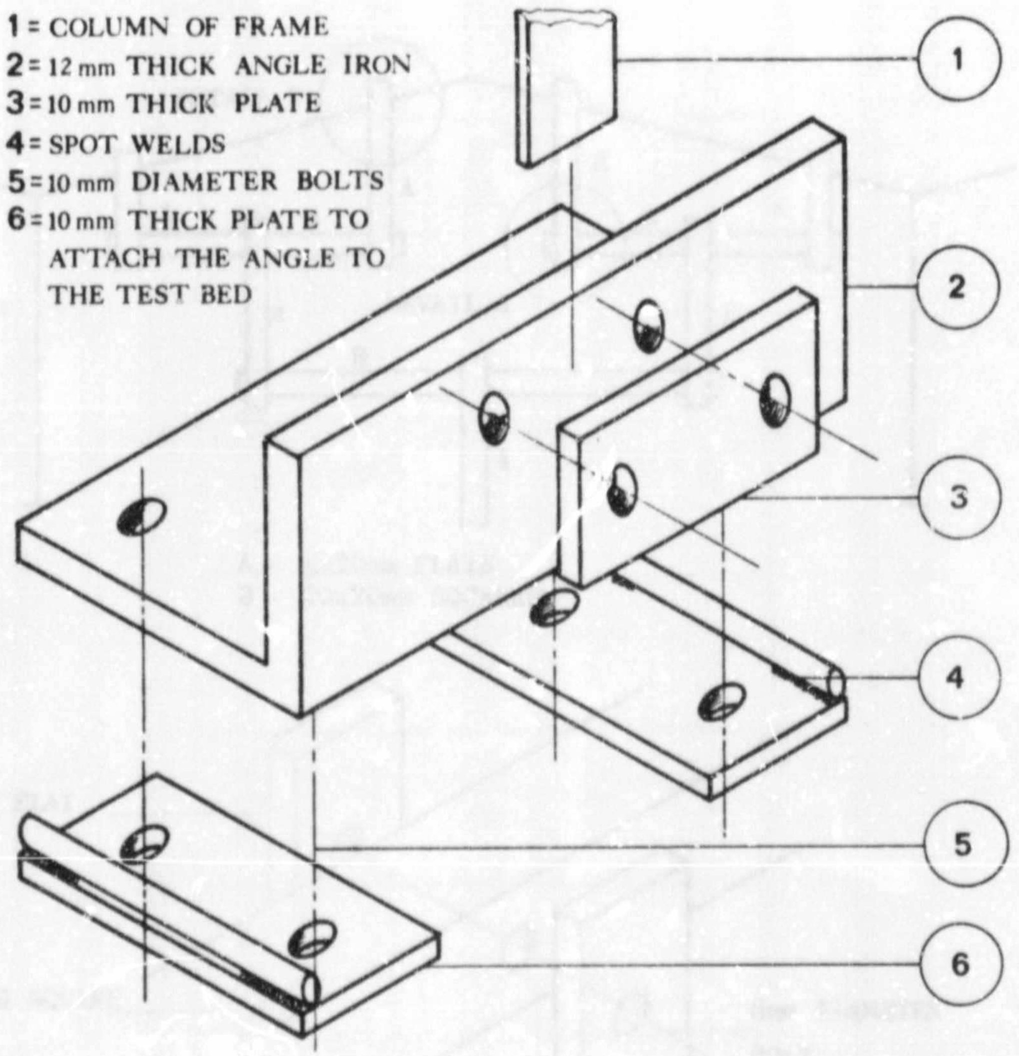

FIGURE 4.4 : BASES USED TO HOLD THE COLUMNS OF THE TEST FRAMES

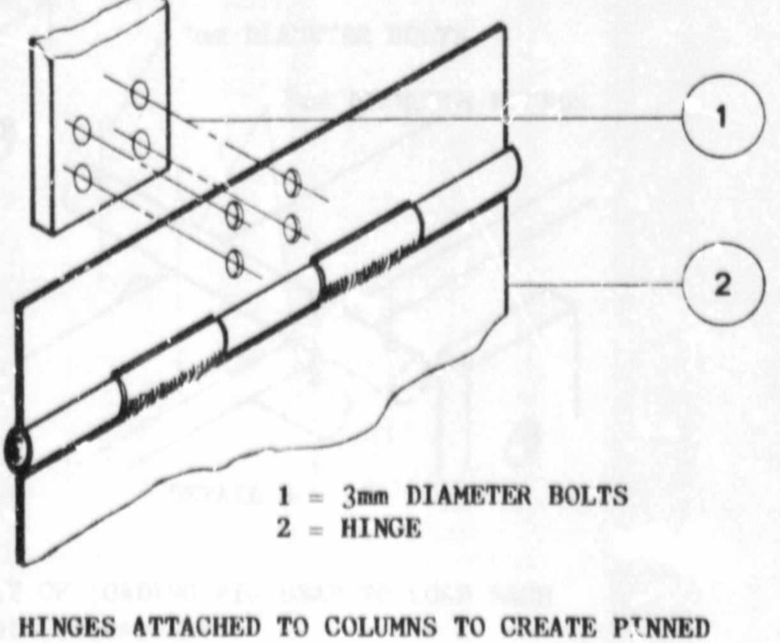

FIGURE 4.5 : HINGES ATTACHED TO COLUMNS TO CREATE PINNED BASES

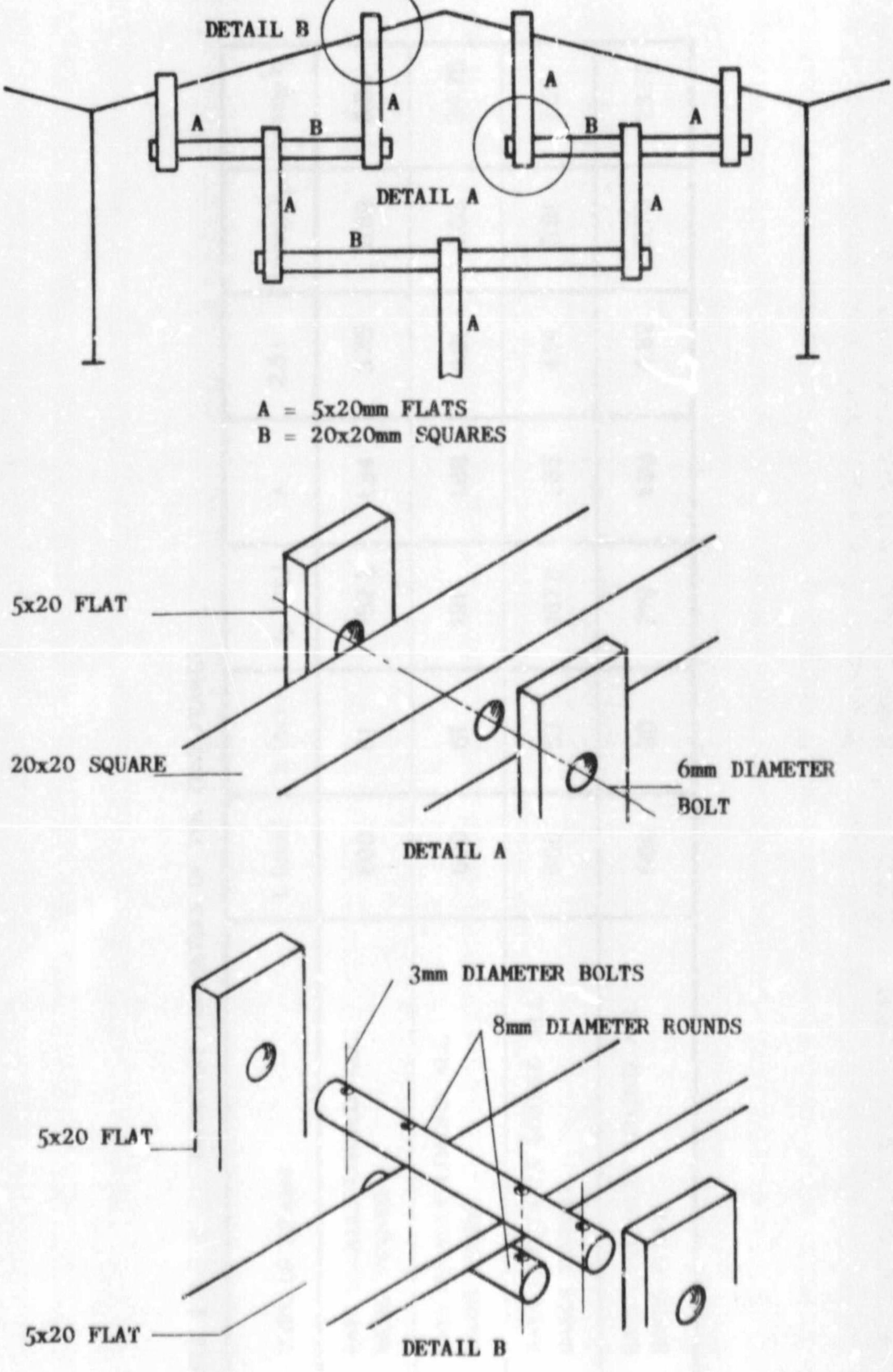

FIGURE 4.6 : LAYOUT OF LOADING RIG USED TO LOAD EACH BAY SIMULTANEOUSLY

TABLE 4.1 : IMPORTANT PARAMETERS OF THE TEST FRAMES

TYPE OF FRAME	L (mm)	h (mm)	P_p (kg)	A	2.5A	$P_{c\,snap}/P_p$	$P_{c\,sway}/P_p$
BAYS EQUALLY LOADED, ALL BASES PINNED	600	61	152.2	1.34	3.35	8.69	6.34
BAYS EQUALLY LOADED, ALL BASES FIXED	600	61	191	1.68	4.21	7.63	34.76
BAYS UNEQUALLY LOADED, ALL BASES PINNED	600	55	187.8	1.65	4.14	5.91	7.35
BAYS UNEQUALLY LOADED, ALL BASES FIXED	600	80	219	1.93	4.82	5.70	23.73

TABLE 4.1 : IMPORTANT PARAMETERS OF THE TEST FRAMES

TYPE OF FRA[illegible]	L (mm)	h (mm)	P_p (kg)	A	[illegible]	$P_{c\,snap}/P_p$	$P_{c\,sway}/P_p$
BAYS EQUALLY LOADED, ALL BASES PINNED	600	61	152.2	1.34	3.35	8.69	6.34
BAYS EQUALLY LOADED, ALL BASES FIXED	600	61	191	1.68	4.21	7.63	34.76
BAYS UNEQUALLY LOADED, ALL BASES PINNED	600	55	187.8	1.65	4.14	5.91	7.35
BAYS UNEQUALLY LOADED, ALL BASES FIXED	600	80	219	1.93	4.82	5.70	23.73

that the strengthening effects of cladding were therefore absent. It has been implied that not more than approximately 10% strength gain should be assigned to cladding and strain hardening.[11] Frames should therefore fail at approximately 90% of the calculated rigid plastic collapse load.

* If the limit of 2,5A is correct, and the frames fail at loads substantially lower than 90% of the plastic collapse load, this suggests that Horne over-estimates the elastic snap-through buckling load of pitched-roof portal frames.
* All the values of $P_{c\ sway}/P_p$ are greater than the proposed limit of 5 and therefore sway instability should not occur. In most cases, the ratio of $P_{c\ snap}/P_p$ is smaller than the ratio of $P_{c\ sway}/P_p$, indicating that snap-through instability will occur before sway. However, in the first case the sway ratio is more serious than the snap-through ratio, so that sway failure may precede snap-through failure. A visual check of the experimental failure will clarify this.

In order to prevent individual member instability the following interaction equation was satisfied for critical members within each frame:[1]

$$\frac{m.Mx}{Max} + \frac{m.My}{May} \leq 1 \qquad (16)$$

m = uniform moment factor obtained from Table 18 in BS 5950

Mx = applied moment about the major axis at the critical section

My = applied moment about the minor axis at the critical section

Max = maximum allowable buckling moment about the major axis in the presence of axial load

May = maximum allowable buckling moment about the minor axis in the presence of axial load

This particular interaction equation found in Clause 4.8.3.3 in BS 5950 gives similar results to equations found in the American and Australian codes, which if satisfied prevent individual member instability in plastic design. Detailed calculations for the case all bays equally loaded, bases pinned are given in appendix F. Similar calculations were done to check member instability in the other frames.

If load-deflection graphs of the test frames are plotted, it is also possible to detect member instability rather than frame instability from these. If a smooth curve becoming asymptotic to the horizontal is obtained frame instability will occur before member stability. If a load-deflection plot, however, indicates that failure has occurred before the curve flattens out, member instability is the cause of failure. This is shown in figure 4.7.

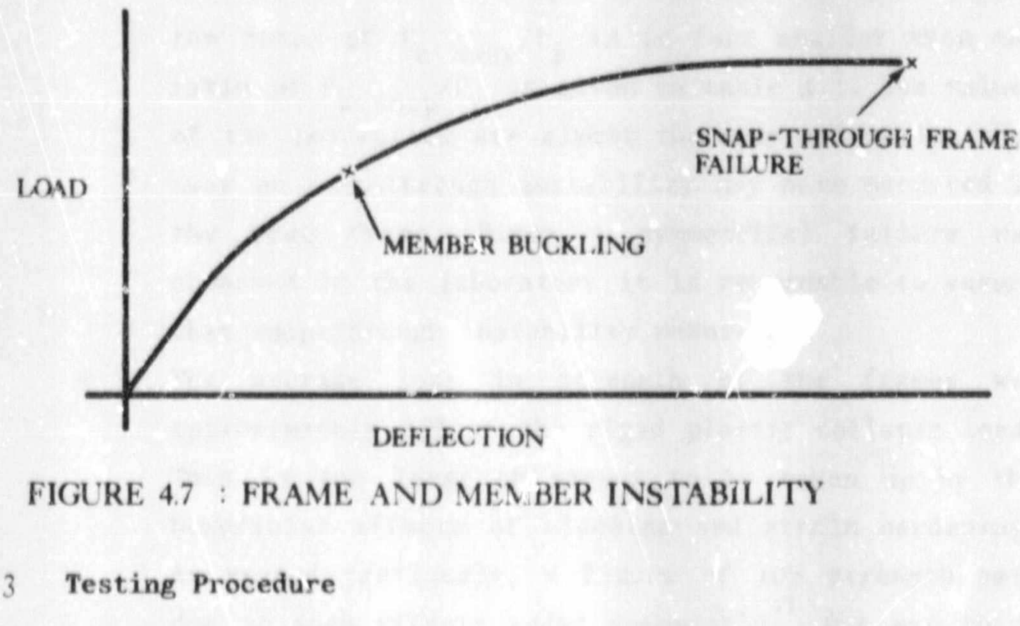

FIGURE 4.7 : FRAME AND MEMBER INSTABILITY

4.3 Testing Procedure

The loading was initially applied in increments of ten to twenty kilograms in each bay, using the loading rig shown in figure 4.6. As the failure load was approached these load increments were reduced considerably.

At each load increment, the apex deflection of the central bay was recorded so that a load-deflection curve for each frame could be drawn. Photographs of each frame were taken periodically. Figure 4.8 gives examples of the many photographs taken. The ultimate failure load in the middle bay was then recorded as a percentage of the simple plastic collapse load of the central bay.

4.4 Test Results

As previously mentioned eight frames were tested. Tables 4.2 to 4.5 give the readings taken during the experiments. Figures 4.9 to 4.12 illustrate the load-deflection curves obtained.

From the results the following conclusions are reached:

* All load-deflection curves obtained are smooth and gradually flatten out. This indicates that member instability did not cause premature failure of any significance in the frames tested.
* For the case all bays equally loaded, all bases pinned the ratio of $P_{c\ sway}/P_p$ is in fact smaller than the ratio of $P_{c\ snap}/P_p$ as given in table 4.1. The values of the two ratios are almost the same indicating that sway or snap-through instability may have occurred in the test frame. Since a symmetrical failure was observed in the laboratory it is reasonable to assume that snap-through instability resulted.
* The average loss in strength of the frames was approximately 25% of the rigid plastic collapse load. This is too large an amount to be taken up by the beneficial effects of cladding and strain hardening. As stated previously, a figure of 10% strength gain due to such effects seems acceptable.[11] One may think that this value of 10 percent is low. However, if the snap-through limit by Horne, $P_{c\ snap}/P_p = 2{,}5A$, is evaluated for the **accurate** elastic snap-through stability buckling load of the bare frame, as intended, a failure load of approximately 0,95 P_p would result for practical frames. Hence the 10 percent expected from strain hardening and cladding seems generous by comparison.

If Horne's proposal of $P_{c\ snap}/P_p \geq 2{,}5A$ is regarded as correct, then in order for such losses to occur the elastic snap-through buckling load must be over-estimated.

A detailed analysis of the results in the following section will establish whether this is indeed so.

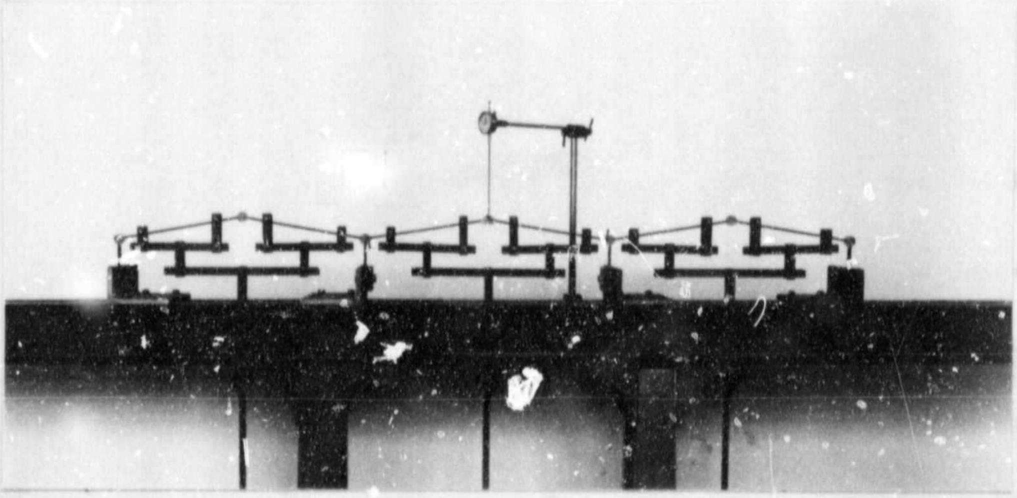

BEFORE LOADING

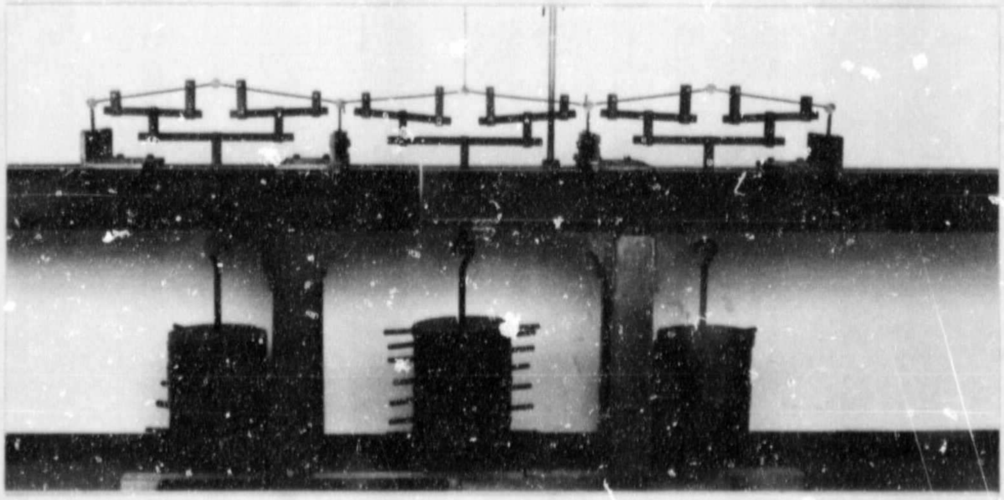

DURING LOADING

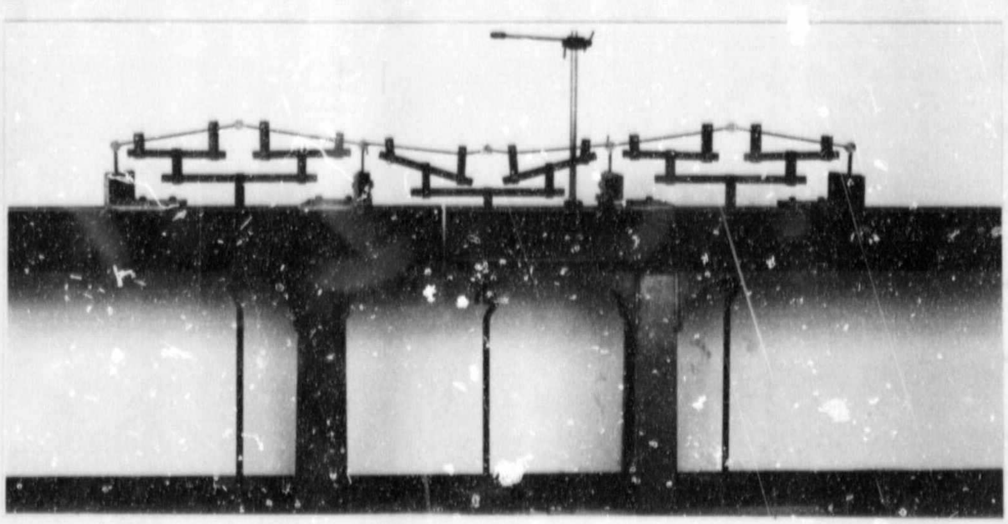

FRAME AFTER FAILURE

FIGURE 4.8: PHOTOGRAPHS SHOWING TESTING OF A FRAME

TABLE 4.2 : LOAD-DEFLECTION RESULTS; ALL BAYS EQUALLY LOADED, ALL BASES PINNED

TEST 1		TEST 2	
LOAD/BAY (kg)	APEX DEFLECTION (mm)	LOAD/BAY (kg)	APEX DEFLECTION (mm)
0	0	0	0
20	1.39	20	1.03
40	3.02	40	2.17
60	4.72	60	3.44
70	5.48	70	4.12
80	6.40	80	4.86
90	7.28	90	5.63
100	8.47	100	6.40
110	11.00	110	8.09
115	14.17	115	10.43
120	19.00	120	14.59
120	22.90	121	17.88
		122	22.00
		123	24.72
PLASTIC COLLAPSE LOAD OF THE CENTRAL BAY = 152.2 kg			
PERCENTAGE OF P_p = 78.84		PERCENTAGE OF P_p = 80.80	

TABLE 4.3 : LOAD-DEFLECTION RESULTS; ALL BAYS EQUALLY LOADED, ALL BASES FIXED

TEST 1		TEST 2	
LOAD/BAY (kg)	APEX DEFLECTION (mm)	LOAD/BAY (kg)	APEX DEFLECTION (mm)
0	0	0	
20	0.50	20	0.44
40	0.94	40	0.90
60	1.44	60	1.34
80	1.98	80	1.77
100	2.92	100	2.60
110	3.60	110	3.28
120	4.33	120	3.98
130	5.05	130	4.65
140	6.27	140	5.79
145	8.00	145	7.70
PLASTIC COLLAPSE LOAD OF THE CENTRAL BAY = 191 kg			
PERCENTAGE OF P_p = 75.9		PERCENTAGE OF P_p = 75.9	

TABLE 4.4 : LOAD-DEFLECTION RESULTS, BAYS UNEQUALLY LOADED, ALL BASES PINNED

TEST 1			TEST 2		
OUTER BAYS (kg)	CENTRAL BAY (kg)	APEX Δ (mm)	OUTER BAYS (kg)	CENTRAL BAY (kg)	APEX Δ (mm)
0	0	0	0	0	0
10	15	0.90	10	15	1.07
20	30	1.85	20	30	2.20
30	45	2.95	30	45	3.39
42	60	3.96	42	60	4.57
52	75	5.20	52	75	5.85
62	90	6.50	62	90	7.27
72	105	7.95	72	105	8.79
80	115	9.20	80	115	9.81
87	125	11.00	87	125	11.30
94	135	13.85	94	135	14.23
94	135	15.90	94	135	18.60
94	135	19.00	94	135	22.65
94	135	39.70			
PLASTIC COLLAPSE LOAD OF THE CENTRAL BAY = 187.8 kg					
PERCENTAGE OF P_p = 71.8			PERCENTAGE OF P_p = 71.8		

TABLE 4.5 : LOAD-DEFLECTION RESULTS; BAYS UNEQUALLY LOADED, BASES FIXED

TEST 1			TEST 2		
OUTER BAYS (kg)	CENTRAL BAY (kg)	APEX (mm)	OUTER BAYS (kg)	CENTRAL BAY (kg)	APEX (mm)
0	0	0	0	0	0
20	30	1.26	20	30	1.50
40	60	2.75	40	60	3.09
62	90	4.52	62	90	4.76
72	105	5.90	72	105	5.73
84	120	7.32	84	120	6.69
94	135	8.59	94	135	8.27
94	135	8.78	101	145	9.32
101	145	10.06	108	155	11.71
108	155	11.47	112	160	14.15
112	160	12.95	114	163	16.63
112	160	13.70			
115	165	16.91			
PLASTIC COLLAPSE LOAD OF THE CENTRAL BAY = 219 kg					
PERCENTAGE OF P_p = 75.3			PERCENTAGE OF P_p = 74.4		

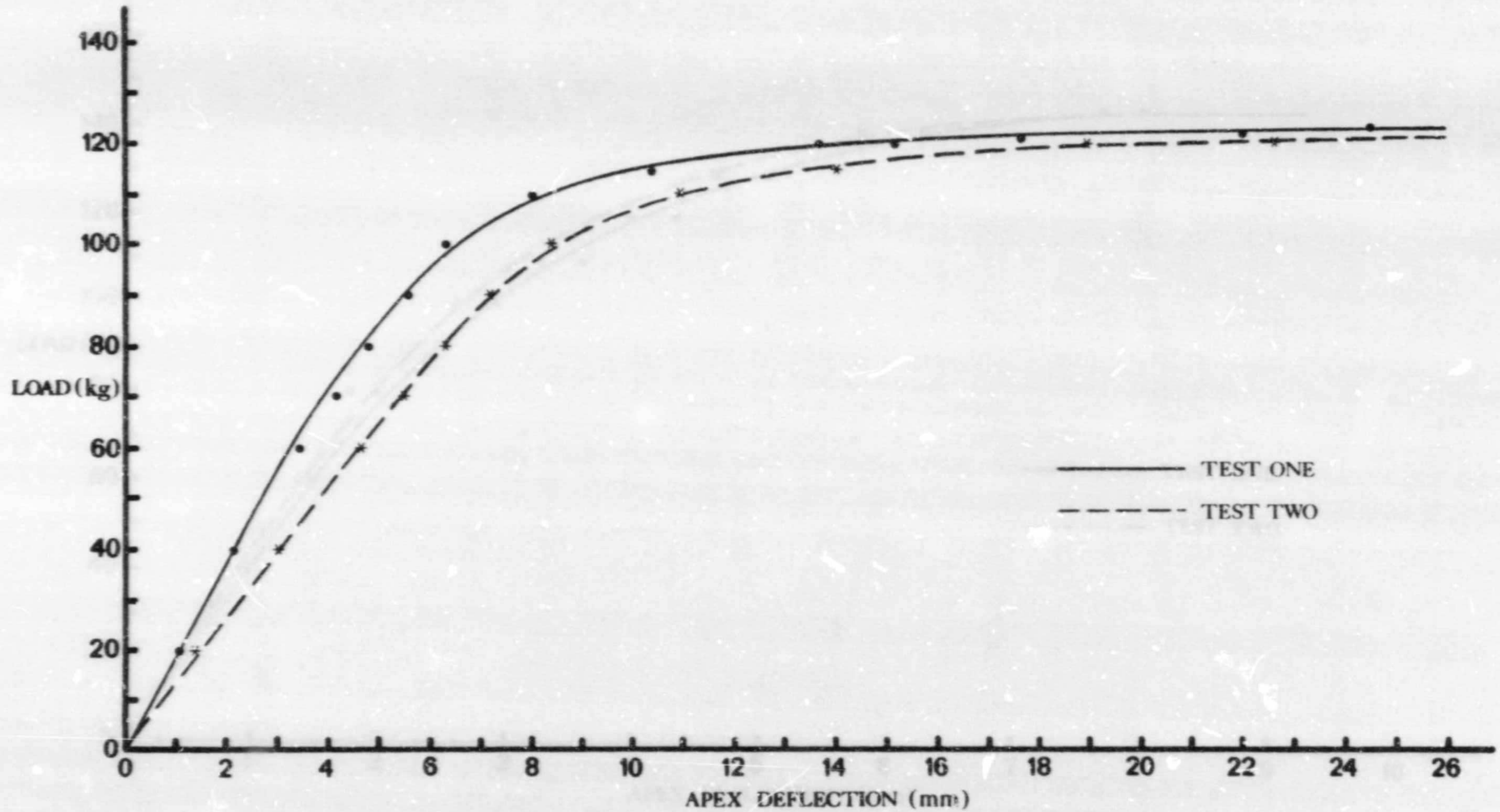

FIGURE 4.9 : LOAD-DEFLECTION GRAPH; BAYS EQUALLY LOADED, BASES PINNED

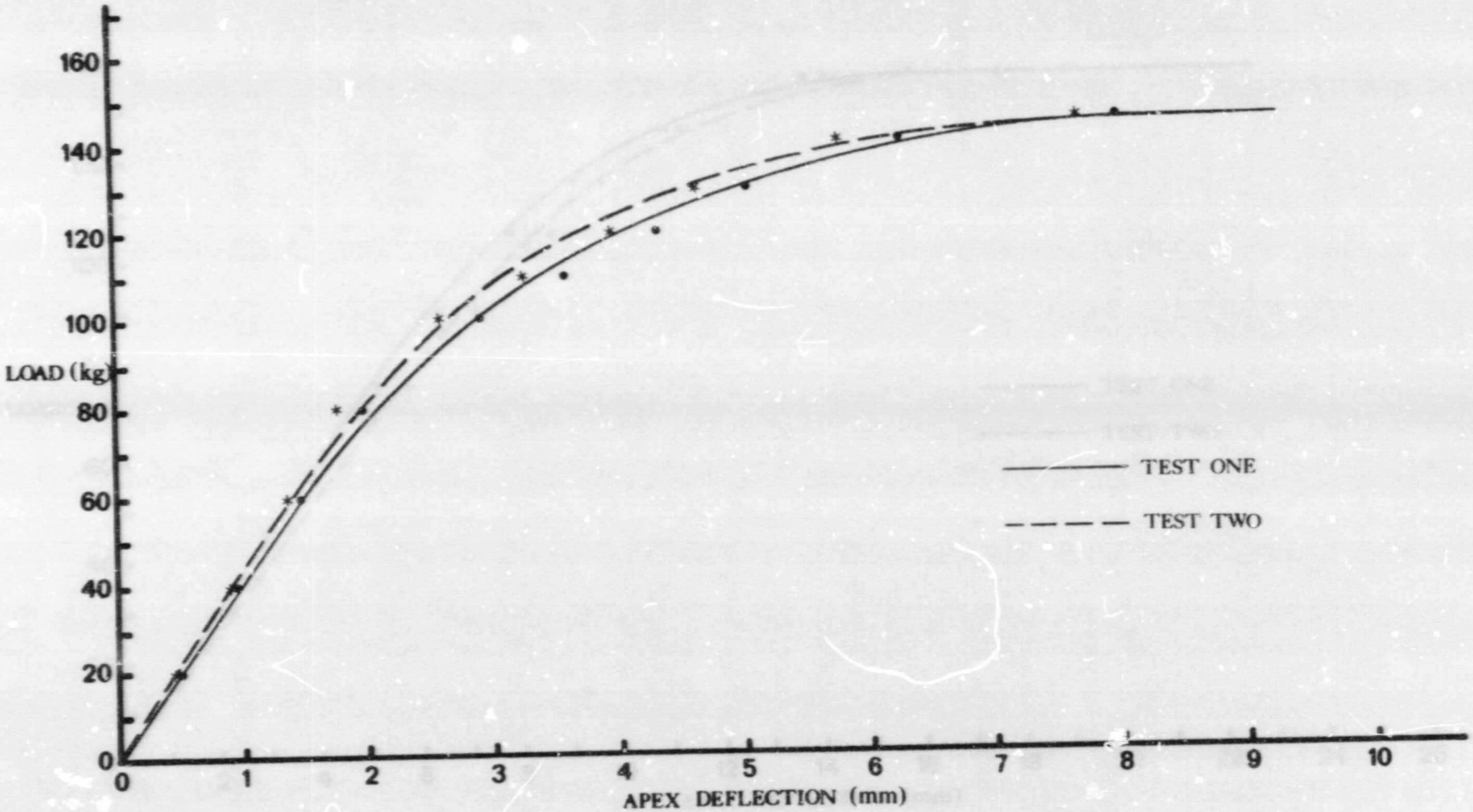

FIGURE 4.10: LOAD - DEFLECTION GRAPH; BAYS EQUALLY LOADED, BASES FIXED